Relationship between structural and functional changes in glaucomatous eyes: A multifocal electroretinogram study

Hiroki Tanaka
Gifu Daigaku Igakubu Daigakuin Igakukei Kenkyuka
Kyoko Ishida (kyoko.ish@gmail.com)
Toho Daigaku Iryo Center Ohashi Byoin https://orcid.org/0000-0001-5141-1000
Kenji Ozawa
Gifu Daigaku Igakubu Daigakuin Igakukei Kenkyuka
Akira Sawada
Gifu Daigaku
Kiyofumi Mochizuki
Gifu Daigaku Igakubu Daigakuin Igakukei Kenkyuka
Tetsuya Yamamoto
Gifu Daigaku Igakubu Daigakuin Igakukei Kenkyuka

Research article

Keywords: multifocal electroretinography, optical coherence tomography, Humphrey Field Analyzer, open angle glaucoma

Posted Date: January 13th, 2020

DOI: https://doi.org/10.21203/rs.2.20694/v1

Version of Record: A version of this preprint was published at BMC Ophthalmology on August 21st, 2021.
See the published version at https://doi.org/10.1186/s12886-021-02061-8.

Abstract

Background: The association between the structure of the macular region and its function as measured by multifocal electroretinography (mfERG) and the mean thresholds (MT) of the visual field (VF) is not well-understood. Methods: The macular retinal nerve fiber layer (mRNFL) and the ganglion cell and inner plexiform layer (GCIPL) in six regions were measured by optical coherence tomography (OCT). For functional assessment, MT and mfERG scans with parameters of the second-order kernel responses within the central 5°, nasal to temporal amplitudes ratio (N/T), and the multifocal photopic negative response to B-wave ratio (mfPhNR/B) were measured. Forty-one glaucoma patients underwent OCT, mfERG, and MT measurement and 55 healthy subjects underwent mfERG.

Results: The mfPhNR/B was significantly smaller ($P < 0.01$) and the N/T was significantly larger ($P < 0.01$) in glaucoma patients than in normal subjects. In glaucoma patients, the N/T is significantly correlated with the thickness of inferior and inferotemporal GCIPL ($r = -0.317$ and -0.360, respectively) and MT of corresponding VF areas ($r = -0.330$ and -0.334, respectively) (all P values < 0.05). The mfPhNR/B was significantly correlated with the thickness of mRNFL in the central area ($r = 0.365$, $P = 0.02$) and with the MT of all corresponding VF areas (r rages between 0.330 and 0.460, all P values < 0.04), except for the inferotemporal area. However, correlation was not observed between the N/T and the mfPhNR/B in any location.

Conclusions: Significant differences exist between glaucoma and healthy participants in the N/T and mfPhNR/B. Correlations were observed between two mfERG parameters and OCT parameters or MT in glaucoma patients. Further research should seek to demonstrate whether the N/T and the mfPhNR/B should be applied in a complementary fashion.

1. Background

Glaucomatous optic neuropathy is associated with the loss of retinal ganglion cells (RGCs) and their axons. The photopic negative response (PhNR) of the full-field electroretinography (ERG) is a slow negative potential following the a- and b-waves that has been reported to originate primarily from the neural activities of the RGCs [1–3]. The amplitudes of the PhNR in focal ERG scans were significantly reduced in eyes with glaucoma [3–6]. However, the PhNR can be measured in several different ways, either as the negative trough following the b-wave or at a fixed time point [7–9]. Wu et al. recently reported that the PhNR to B-wave ratio (PhNR/B; B-wave amplitude defined as the a-wave trough to b-wave peak) exhibited the lowest magnitude of test–retest variability and concluded that PhNR/B was the optimal measure of the PhNR [10].

In earlier reports, the nasal to temporal amplitudes ration (N/T) of the first slice of the second-order kernels of multifocal electroretinography (mfERG) scans measured within 5° of the macula was smaller in glaucoma patients than in normal subjects. Further, a significant correlation was present between N/T and visual field (VF) parameters or the retinal thickness in the inferior quadrant in eyes with moderate

glaucoma [11, 12]. These findings suggest that PhNR/B and N/T might be helpful in determining functional defects in patients with glaucoma.

There are several reports available outlining direct comparisons among visual sensitivities determined by standard automated perimetry (SAP), structural parameters of the inner retina obtained by optical coherence tomography (OCT), and the amplitude of the PhNR/B or the N/T [4, 5, 13–15], but no reports especially conducting comparisons between N/T and the PhNR/B of mfERG scans (mfPhNR/B) in the same glaucoma patient have been published.

Thus, this study sought to investigate the association between the morphological statuses of the macular region by OCT, the functional status including two mfERG parameters with N/T and mfRhNR/B, and the sensitivities of SAP in the same glaucoma patients.

2. Materials And Methods

2.1. Subjects

This was an observational cross-sectional study of patients treated at the Glaucoma Service of the Gifu University Hospital over a six-year period. We obtained written informed consent from all participants and all of the procedures conformed to the tenets of the Declaration of Helsinki. The Institutional Board of Research Associates of Gifu University Graduate School of Medicine approved our research protocols.

Open angle glaucoma (OAG) diagnoses were based on the presence of normal open-angle and glaucomatous optic nerve changes corresponding to VF defects. We classified the patients as having normal tension glaucoma (NTG) if none of the recorded intraocular pressures (IOPs) exceeded 21 mmHg in either eye at all examinations, while the remaining patients were classified as having primary OAG (POAG). Patients eligible for study inclusion had clinical diagnoses of POAG or NTG, a refractive spherical equivalent ranging between − 6.0 diopters (D) and + 3.0 D, and a best-corrected visual acuity (VA) of 0 logarithm of the minimum angle of resolution (logMAR) units or less.

We excluded patients with intraocular abnormalities other than glaucoma; those with significant cataracts that could induce refractive or VF errors; those with a history of any medication use that could affect the pupillary diameter, those with intraocular surgeries including laser therapy; and those with medical treatment changes in the interval among the VF tests, OCT examinations, and mfERG recordings. All examinations including VF, OCT, and mfERG were performed each other within six months.

Normal participants were included who had refractive spherical equivalents of between − 6.0 D and + 3.0 D and best-corrected VA of 0 logMAR units or less, no family history of glaucoma, a normal-appearing optic nerve head with an intact neuroretinal rim and retinal nerve fiber layer (RNFL), and IOPs of less than 21 mmHg without a history of elevated IOP. We excluded subjects who had any of the following conditions: history of intraocular surgery, intraocular eye disease, or an inability to clinically view the optic discs due to media opacity or poorly dilating pupils.

2.2. OCT

Pupils were dilated with topical 0.5% tropicamide and 0.5% phenylephrine (Mydrin-P®; Santen Pharmaceutical, Osaka, Japan) before the OCT examinations with a Cirrus high-definition OCT (HD-OCT) 4000 instrument (Carl Zeiss Meditec, Jena, Germany). The software automatically collected measurements of the peripapillary RNFL with a diameter of 3.46 mm consisting of 256 A-scans centered on the optic disc. We obtained the average thickness of the circumpapillary RNFL (cpRNFL), then used the Macula Cube 200 × 200 and Ganglion Cell Analysis (GCA) programs to collect additional data in glaucoma patients as follows.

The macular cube scan generated one set of 200 horizontal B-scans, each composed of 200 A-scans centered on a 6- × 6-mm macular region. The built-in GCA algorithm (Cirrus H-OCT software, version 6.0) measured the thicknesses of the macular RNFL (mRNFL) and ganglion cell-inner plexiform layer (GCIPL) within a 6- × 6- × 2-mm cube in an elliptical annulus around the fovea. By using the GCA algorithm, the GCIPL thickness was calculated automatically as the distance from the outer boundary of the RNFL to the outer boundary of the inner plexiform layer (IPL) and stratified such as global, minimum, and sectoral values (i.e., superonasal, superior, superotemporal, inferotemporal, inferior, and inferonasal sectors) (Fig. 1a). We also measured the mRNFL thickness as the distance between the internal limiting membrane and the outer boundary of the RNFL and calculated the same six sectorial values. We only incorporated OCT images with a high quality of signal strength greater than 7/10 in our analysis.

2.3. VF testing

All glaucoma participants underwent perimetric examinations using the Humphrey Field Analyzer (HFA) (750 I series; Carl Zeiss Meditec, Jena, Germany) with the Central 30 − 2 (HFA 30 − 2) and the Central 10 − 2 programs (HFA 10 − 2) using the Swedish Interactive Threshold Algorithm. We identified glaucomatous VF defects by the presence of three or more significant ($P < 0.05$) non−edge-contiguous points, with at least one point located at the $P < 0.01$ level in the pattern deviation plot along with grading outside the normal limits in the glaucoma hemifield test. VF tests were considered reliable when false-negative responses were less than 15%, false-positive responses were less than 15% and fixation losses were less than 20%. Based on the report of RGC displacement, we classified the stimulus points on the HFA 10 − 2 corresponding to the six sectors of the GCIPL measurement ellipse into six groups (Fig. 1b) [16]. We averaged the thresholds of each sector on the SAP.

2.4. mfERG scans

Both glaucoma patients and normal subjects underwent mfERG. We used the Visual Evoked Response Imaging System Science (VERIS) 5.1.10× (Electro-Diagnostic Imaging, Milpitas, CA, USA) to record mERG scans according to a published method [11, 12, 14]. After pupils were dilated to at least 8 mm in diameter with Mydrin-P®, we placed a bipolar contact lens electrode (Mayo, Inazawa, Japan) on the anesthetized (oxybuprocaine hydrochloride, Benoxil®; Santen Pharmaceutical, Osaka, Japan) cornea. We covered the contralateral eye, and then applied hydroxyethylcellulose gel (Scopisol®; Senju Pharmaceutical, Osaka,

Japan) to the cornea to protect it from dehydration and to achieve good electrical contact between the electrodes and the cornea. We attached a gold-cup electrode to the right earlobe as a ground electrode. We then carried out refractions to elucidate the patients' best VA for the stimulus viewing distance. Next, we adjusted the viewing distance to compensate for changes in the retinal image size due to the refractive lens used. During the mfERG recordings, the subjects sat with their chin and forehead tightly fixed. We instructed the subjects to fixate on a point at the center of the cathode ray tube (CRT) monitor while the eyes were being stimulated. The distance from the tested eye to the CRT monitor was 33 cm at zero diopters. The amplitudes of the mfERG were expressed as the response density, nV/deg^2, or μV, representing the amplitudes as a function of the stimulus area.

2.4. 1. P1 Component of the first slice of second-order kernels of mfERG scans

The visual stimuli consisted of 37 hexagons that were displayed on a monochrome computer monitor (QB1781; Chuomusen, Tokyo, Japan) (Fig. 2a). The stimulus array subtended a visual angle of 50° by 40°. Each hexagonal element of the stimulus was independently alternated between black (5 cd/m^2) and white (200 cd/m^2; contrast: 95.1%) at a frame rate of 75 Hz according to a binary m-sequence. We set the bandpass filters at 10 to 300 Hz. We monitored the positions of the eyes during the recordings through the VERIS recording window. Each recording lasted approximately four minutes, and we discarded segments with eye movements or blinking artifacts and recorded them again. We applied an artifact elimination technique once, with no spatial smoothing [17]. We studied the amplitudes of the first positive peak, P1 (Fig. 2b). The P1 amplitudes of the first slice of the second-order kernel responses were measured according to a published method [11, 12, 14].

2.4.2. Nasal to temporal amplitude ratio analyses of mfERG scans

The mfERG scans elicited by the 37-hexagon stimulus array within a circle of a 5° radius are shown in Fig. 2a. We compared the summed mfERG scans from the central 5° of the nasal VF (i.e., temporal hemisphere of the central 5° retinal area; red color in Figs. 2a and 2c) with those in the temporal hemisphere of the central 5° VF (i.e., nasal hemisphere of the central 5° retinal area; orange color in Figs. 2a and 2c). We calculated the N/T—namely, the ratio of the mfERG P1 amplitudes of the first slice of the second-order kernel (Fig. 2b)—in the nasal hemisphere of the VF (i.e., temporal hemisphere of the retina) and compared with that in the temporal hemisphere of the VF (i.e., nasal hemisphere of the retina) in the central 5°. We also calculated the correlations between the thresholds obtained from the corresponding VF area, OCT parameters, and the N/T.

2.4.3. Multifocal photopic negative response

The mfPhNRs were elicited by a circular stimulus with a 5° radius centered on the fovea and by a quarter of an annulus placed in the superotemporal, superonasal, inferotemporal, and inferonasal regions around the fovea (Fig. 3a). The radius of the inner border of the annulus was 5° and that of the outer border was 20°. White (200 cd/m^2) or black (5 cd/m^2) elements were presented in a pseudorandom binary m-sequence at a frequency of 37.5 Hz. Each recording lasted approximately two minutes. A steady background surrounded the stimulus field. We measured the multifocal a-wave amplitude from the baseline to the trough of the first negative response and the multifocal B-wave (mfB-wave; P1–N1) from the first negative trough to the peak of the following positive wave [18]. The PhNR was measured from the baseline to the negative trough at more than 70 ms from the stimulus onset (Fig. 3b) [6].

2.4.4. mfPhNR/B analyses

We calculated the amplitudes of the mfPhNR/B in each sector. To compare the mfPhNR/B with the corresponding VF findings, we measured the thresholds with the HFA 30 − 2 and averaged for the same sectors according to the distance from the macula within the central 20° (Fig. 4). We also calculated the correlations between the thresholds of the corresponding VF area, the mfPhNR/B, and OCT parameters.

2.5. Statistical analyses

For cases in which both eyes met all eligibility criteria, we chose one eye randomly for the statistical analyses. We used the Mann–Whitney U and chi-squared tests to compare the values between normal participants and glaucoma patients and between NTG and POAG. The Kruskal–Wallis test was deployed to compare the differences in sectorial values of OCT parameters, VF sensitivities, and mfERG. We used Spearmann rank correlation coefficients to assess associations among data of VF, OCT, and mfERG scans. A P-value of less than 0.05 was considered statistically significant. We performed all statistical analyses using the Statistical Package for the Social Sciences version 16.0 software program (IBM Corp., Armonk, NY, USA).

3. Results

3.1. Demographic data of glaucoma patients

The demographics of the 41 eyes of 41 patients with OAG included in this study are presented in Table 1. The mean patient age was 58.9 years, while the mean IOP for all eyes was 13.9 mmHg. Ten patients had POAG and 31 had NTG. Nineteen patients were using topical antiglaucoma medications (NTG: 12 patients; POAG: 7 patients). We found no significant difference in mean IOP between patients with POAG (15.3 ± 2.6 mmHg) and those with NTG (13.5 ± 2.5 mmHg) (P = 0.09). The mean deviation (MD) for all patients obtained with the HFA 30 − 2 was − 7.66 dB and the pattern standard deviation (PSD) was 9.69 dB. Similarly, the MD with the HFA 10 − 2 program was − 7.22 dB and the average PSD was 8.45 dB. The mean cpRNFL thickness was 68.6 μm.

Table 1
The Demographic data of glaucoma patients

Gender (male/female)	**22 eyes/19 eyes**
Eye (Right/Left)	22 eyes/19 eyes
Age [years]	58.9 ± 11.0 (35 ~ 78)
Type of Glaucoma (POAG/NTG)	10 eyes/31 eyes
Corrected Visual acuity (Log MAR)	-0.13 ± 0.07 (-0.18 ~ 0.00)
Spherical Equivalent [Diopters]	-1.92 ± 2.40 (-5.88 ~ + 2.88)
Intraocular Pressure [mmHg]	13.9 ± 2.7 (10 ~ 21)
HFA Central 30 − 2 Program	
Mean Deviation [dB]	-7.66 ± 7.06 (-29.26 ~ 2.02)
Pattern Standard Deviation [dB]	9.69 ± 5.28 (1.61 ~ 18.76)
HFA Central 10 − 2 Program	
Mean Deviation [dB]	-7.22 ± 7.11 (-27.42 ~ 2.07)
Pattern Standard Deviation [dB]	8.45 ± 5.64 (0.98 ~ 17.19)
Circumpapillary retinal nerve fiber layer thickness [μm]	68.6 ± 11.9 (46 ~ 100)
POAG: primary open angle glaucoma	
NTG: normal tension glaucoma	
LogMAR: Logarithm of the minimum angle of resolution (	
HFA: Humphrey Field Analyzer	
Values are mean ± standard deviation (range)	

3.2. Comparisons of clinical and mfERG parameters between glaucoma and normal participants

The mfPhNR/B was measured in 26 eyes of 26 normal subjects and 41 eyes of 41 glaucoma patients, respectively. Although the clinical backgrounds of the populations were not statistically different except for with respect to refraction, glaucoma patients showed significantly lower values of mfPhNR/B in all measurement sectors relative to normal subjects (all $P < 0.05$) (Table 2).

Table 2

Comparisons of clinical and mfERG parameters between glaucoma and normal participants

		Glaucoma	Normal			
			mfPhNR/B measurement	**P-value**	**N/T measurement**	**P-value**
Gender (male/female)		22 /19	13 /13	0.770	10/19	0.113
Eye (Right/Left)		22/19	11/15	0.365	16/13	0.900
Age [years]		58.9 ± 11.0 (35 ~ 78)	62.9 ± 15.7 (20 ~ 78)	0.067	57.4 ± 10.1 (43 ~ 75)	0.471
Spherical Equivalent [Diopters]		-1.92 ± 2.40 (-5.88 ~ + 2.88)	-0.75 ± 2.22 (-5.00 ~ + 2.63)	0.036	-0.31 ± 1.84 (-4.75 ~ + 2.25)	0.004
mfPhNR/B	Center	0.34 ± 0.13 (0.14 ~ 0.77)	0.43 ± 0.13 (0.26 ~ 0.93)	0.001		
	Superotemporal	0.21 ± 0.08 (0.07 ~ 0.45)	0.26 ± 0.07 (0.15 ~ 0.38)	0.003		
	Superonasal	0.21 ± 0.06 (0.10 ~ 0.41)	0.27 ± 0.06 (0.18 ~ 0.37)	0.000		
	Inferonasal	0.25 ± 0.07 (0.12 ~ 0.42)	0.31 ± 0.07 (0.16 ~ 0.45)	0.001		
	Inferotemporal	0.25 ± 0.08 (0.12 ~ 0.47)	0.31 ± 0.07 (0.17 ~ 0.42)	0.005		
N/T		0.85 ± 0.27 (0.41 ~ 1.58)			0.58 ± 0.17 (0.15 ~ 0.87)	0.000
mfERG: multifocal electroretinogram						
mfPhNR/B: multifocal photopic negative response to B-wave ratio						
N/T: nasal to temporal amplitude ratio						
Values are mean ± standard deviation (range)						
Bolded numbers are statistically significant (P < 0.05)						

Separately, the N/T was measured in 29 eyes of 29 normal subjects and 41 eyes of 41 glaucoma patients (Table 2). Glaucoma patients had significantly higher N/T (P

= 0.000) and less myopia (P = 0.004) than normal subjects.

3.3. The mean GCIPL and mRNFL thicknesses measured by OCT, the mean threshold of HFA 10 − 2, and the correlations between them in each sector in glaucoma patients

The mean GCIPL and mRNFL thicknesses in the macular sector corresponding to the superonasal VF (Table 3) were the thinnest among the six sectors ($P < 0.01$). The mean thresholds (MT) in the superior and superonasal sectors were lower than those in the inferior hemifields (all $P < 0.01$). The MT in the macular region were significantly correlated with the corresponding sectors of the mean GCIPL thickness (all $P \leq 0.011$; correlation coefficient range: 0.395–0.777), except for the inferotemporal VF sector, which corresponded to the superonasal retina.

Table 3

The mean GCIPL and mRNFL thicknesses measured by OCT, the mean threshold of HFA 10 − 2, and the correlations between them in each sector in glaucoma patients

Sectors	Sectorial Retinal Thickness of OCT		HFA 10 − 2	GCIPL vs HFA10-2		mRNFL vs HFA10-2	
	GCIPL [μm]	mRNFL [μm]	Mean Threshold [dB]	r	P-value	r	P-value
Superotemporal	69.1 ± 10.6 (38 ~ 88)	31.1 ± 9.0 (10 ~ 45)	27.9 ± 8.4 (0 ~ 37.2)	0.487	0.001	0.635	0.000
Superior	62.8 ± 9.1 (49 ~ 86)	23.3 ± 10.0 (10 ~ 41)	20.7 ± 13.5 (0 ~ 36.8)	0.777	0.000	0.890	0.000
Superonasal	60.5 ± 9.61 (46 ~ 85)	15.4 ± 5.5 (8 ~ 26)	23.9 ± 12.2 (0.2 ~ 36.0)	0.744	0.000	0.690	0.000
Inferonasal	67.9 ± 8.7 (49 ~ 88)	19.1 ± 4.7 (7 ~ 29)	31.6 ± 6.1 (5.4 ~ 37.2)	0.424	0.006	0.303	0.054
Inferior	70.2 ± 10.6 (33 ~ 88)	31.3 ± 6.4 (14 ~ 46)	31.0 ± 5.7 (6.5 ~ 36.5)	0.395	0.011	0.345	0.027
Inferotemporal	73.8 ± 11.2 (38 ~ 91)	34.7 ± 6.3 (17 ~ 50)	31.7 ± 4.7 (10.2 ~ 36.2)	0.263	0.097	0.196	0.220
P-value[a]	< 0.000	< 0.000	< 0.000				
GCIPL: Ganglion cell-inner plexiform layer							
mRNFL: Macular retinal nerve fiber layer							
OCT: Optical coherence tomography							
HFA 10 − 2: Humphrey Field Analyzer Program Central 10 − 2							
[a] Kruskal-Wallis test							
r: Spearman rank correlation coefficients							
Values are mean ± standard deviation (range).							
Bolded numbers are statistically significant (P < 0.05)							

The MT also significantly correlated with the corresponding sector of the mRNFL thickness (all $P \leq 0.027$; correlation coefficient range: 0.345–0.890), except for the inferotemporal and inferonasal VF sectors, which corresponded to the superonasal and superotemporal retina.

3.4. Correlation between the N/T of mfERG, the macula thickness of OCT, and the mean thresholds of HFA 10 − 2 in each sector in glaucoma patients

The N/T was significantly correlated with the thickness of the GCIPL in the superior and superonasal sectors ($r = -0.317$; $P = 0.043$ and $r = -0.360$; $P = 0.021$, respectively), which corresponded to the inferior and inferotemporal sectors of the retina (Table 4).

Table 4

Correlation between the N/T of mfERG, the macula thickness of OCT, and the mean thresholds of HFA 10 − 2 in each sector in glaucoma patients

OCT and HFA		**vs N/T**	
Parameter	Sectors	r	P-value
GCIPL of OCT	Average	-0.261	0.099
	Minimum	-0.269	0.089
	Superotemporal	-0.243	0.126
	Superior	-0.317	0.043
	Superonasal	-0.360	0.021
	Inferonasal	-0.030	0.854
	Inferior	-0.074	0.648
	Inferotemporal	-0.094	0.560
mRNFL of OCT	Average	-0.309	0.049
	Minimum	-0.208	0.191
	Superotemporal	-0.249	0.116
	Superior	-0.338	0.031
	Superonasal	-0.270	0.088
	Inferonasal	-0.049	0.759
	Inferior	-0.042	0.794
	Inferotemporal	-0.053	0.742
Mean thresholds of HFA 10 − 2	Mean Deviation	-0.452	0.003

N/T: nasal to temporal amplitude ratio

mfERG: multifocal electroretinogram

OCT; Optical coherence tomopraphy

HFA 10 − 2: Humphrey Field Analyzer Program Central 10 − 2

GCIPL: Ganglion cell-inner plexiform layer

RNFL: Macular retinal nerve fiber layer

r: Spearman rank correlation coefficients

OCT and HFA		vs N/T	
	Superotemporal	-0.222	0.164
	Superior	-0.330	0.035
	Superonasal	-0.334	0.033
	Inferonasal	-0.028	0.862
	Inferior	-0.048	0.768
	Inferotemporal	-0.078	0.626
N/T: nasal to temporal amplitude ratio			
mfERG: multifocal electroretinogram			
OCT; Optical coherence tomopraphy			
HFA 10 − 2: Humphrey Field Analyzer Program Central 10 − 2			
GCIPL: Ganglion cell-inner plexiform layer			
RNFL: Macular retinal nerve fiber layer			
r: Spearman rank correlation coefficients			

The N/T was significantly correlated with the thickness of the mRNFL in the superior sector (r = − 0.338; P = 0.031), which corresponded to inferior sectors of the retina and with the average thickness of the mRNFL (r = − 0.309; P = 0.049). The N/T significantly and negatively correlated with the MT in the superior and the superonasal sectors (r = − 0.330; P = 0.035 and r = − 0.334; P = 0.033, respectively) and with the MD (r = − 0.452; P = 0.003).

3.5. The mfPhNR/B of mfERG, the mean threshold of HFA 30 − 2, and the correlations between them in each sector in glaucoma patients

The amplitudes of the mfPhNR/B and the MT in the superior hemifield (i.e., inferior retinal area) were lower than those in the inferior hemifield (i.e., superior retinal area) (both $P < 0.01$) (Table 5). The mfPhNR/B significantly correlated with the MT of all corresponding areas (all $P \leq 0.035$, correlation coefficient range: 0.330–0.460) except for the inferotemporal VF sector, which corresponded to the superonasal sector of the retina.

Table 5
The mfPhNR/B of mfERG, the mean threshold of HFA 30 − 2, and the correlations between them in each sector in glaucoma patients

Sectors	mfPhNR/B of mf ERG	Mean Threshold [dB] of HFA 30 − 2	r	P-value
Center	0.34 ± 0.13 (0.14 ~ 0.77)	26.1 ± 7.2 (9.8 ~ 35.5)	0.421	0.006
Superotemporal	0.21 ± 0.08 (0.07 ~ 0.45)	19.8 ± 8.8 (2.2 ~ 32.4)	0.417	0.007
Superonasal	0.21 ± 0.06 (0.10 ~ 0.41)	18.9 ± 11.8 (0.0 ~ 33.1)	0.460	0.002
Inferonasal	0.25 ± 0.07 (0.12 ~ 0.42)	23.0 ± 10.5 (0.6 ~ 33.1)	0.330	0.035
Inferotemporal	0.25 ± 0.08 (0.12 ~ 0.47)	23.8 ± 6.3 (0.0 ~ 29.4)	0.289	0.067
P-value[a]	< 0.000	0.004		
mfPhNR/B: multifocal photopic negative response to multifocal B-wave ratio				
mfERG: multifocal electroretinogram				
HFA 30 − 2: Humphrey Visual Field Analyzer Program Central 30 − 2				
Values are mean ± standard deviation (range)				
[a] Kruskal-Wallis test				
r: Spearman rank correlation coefficient				

3.6. Correlations between the mfPhNR/B of mfERG in each sector and the average of the GCIPL and mRNFL of OCT in glaucoma patients

The mfPhNR/B was significantly correlated with the average thickness of the mRNFL in the central area (r = − 0.365; P = 0.019) (Table 6).

Table 6
Correlations between the mfPhNR/B of mfERG in each sector and the average of the GCIPL and mRNFL of OCT in glaucoma patients

Sctors of PhNR/B	vs GCIPL average		vs mRNFL average	
	r	P-value	r	P-value
Center	-0.275	0.082	0.365	0.019
Superotemporal	0.183	0.253	0.199	0.213
Superonasal	0.147	0.358	0.281	0.075
Inferonasal	0.116	0.470	0.191	0.232
Inferotemporal	0.017	0.918	0.051	0.753
mfPhNR/B: multifocal photopic negative response to multifocal B-wave ratio				
mfERG: multifocal electroretinogram				
OCT; Optical coherence tomopraphy				
GCIPL: Ganglion cell-inner plexiform layer				
mRNFL: Macular retinal nerve fiber layer				
r: Spearman rank correlation coefficient				

3.7 Correlation between the N/T and sectorial values of the mfPhNR/B of the mfERG in glaucoma patients

Correlation was not observed between the N/T and the mfPhNR/B in any location (Table 7).

Table 7
Correlation between the N/T and sectorial values of the mfPhNR/B of the mfERG in glaucoma patients

Sectors of mfPhNR/B	N/T	
	r	P-value
Center	-0.054	0.739
Superotemporal	-0.271	0.087
Superonasal	-0.264	0.095
Inferonasal	-0.194	0.225
Inferotemporal	-0.078	0.628
N/T: nasal to temporal amplitude ratio		
mfPhNR/B: multifocal photopic negative response to multifocal B-wave ratio		
mfERG: multifocal electroretinogram		
r: Spearman rank correlation coefficient		

4. Discussion

In the current study, significant differences were found to exist between glaucoma and healthy participants in terms of the N/T and the mfPhNR/B. Moreover, correlations were observed between two mfERG parameters and OCT parameters or MT in glaucoma patients. However, no correlations were found between N/T and the mfPhNR/B in individual glaucoma patients.

In this study, the P1 component of the first slice of the second-order kernel response was elicited by the stimuli in the central 5° region in OAG patients (Fig. 2). However, we adopted the N/T instead of the P1 component because the latter boasts relatively large intersubject variations [12].

The nasal-temporal asymmetry of the mfERG scans is affected in glaucomatous eyes [11, 12]. We previously reported significant differences existed in the N/T of the first slice of the second-order kernel of the mfERG scans in the central 5° between normal and NTG eyes and found significant correlations between the N/T and the MT obtained with the HFA 30 − 2 and 10 − 2 results [11, 14], findings which are in agreement with the current study. The N/T was significantly different between normal subjects and glaucoma patients (Table 2). Moreover, the N/T was significantly and negatively correlated with the MT in the superior and the superonasal sectors and with the HFA 10 − 2 MD in glaucoma patients (Table 4).

In the current study, we used not only the N/T of mfERG scans and HFA 10 − 2 but also OCT parameters and, furthermore, we classified the stimulus points on the HFA 10 − 2 as corresponding to each of six

GCIPL measurement ellipse sectors into six groups (Fig. 1) based on the report of RGC displacement [16]. Although macular ganglion cell complex (GCC) thickness can predict function within the central area in eyes with glaucoma, adjusting for the RGC displacements is essential in evaluating the association between structure and function in the macula [19]. We found statistically significant correlations between the MT and the thicknesses of the GCIPL in all sectors except in the inferotemporal VF sector, which corresponds to the superonasal retina (Table 3). Both relationships—between N/T and MT and between N/T and GCIPL thickness—had significant correlations in the superior and superonasal VF sectors (i.e., inferior and inferotemporal retinal areas) (Table 4). We also found statistically significant correlations exist between the mRNFL thickness and the MTs (Table 3) or N/T (Table 4) in the superior VF sector (i.e., inferior retinal area). These findings may be related to unique glaucomatous VF defect patterns found in the superior and superonasal areas that correspond to inferior and inferotemporal retinal damages [16]. Lee et al. reported that progressive GCIPL thinning in the temporal sector occurred faster in affected than in unaffected hemifields [16]. Na et al. found that the macula cube volume and the thicknesses of the temporal and inferior macular sectors decreased faster in progressively glaucomatous eyes [20]. These reports are in agreement with our findings.

The nasal amplitudes in the first slice of the second-order kernel of mfERG within 5° were significantly smaller than the temporal amplitudes in normal subjects [11, 12], whereas the difference became smaller and thus the N/T ratio became larger (approaching 1.0) after glaucoma development and progression. If the difference in amplitude became insignificant (i.e., saturated) in a very early stage of glaucoma, the ratio reached 1.0 in the early stage of glaucoma progression and, thus, the N/T was not useful clinically for monitoring glaucomatous functional change; however, the nasal amplitudes were still significantly smaller than the temporal amplitudes (4.9 nV/deg^2 in the nasal vs. 5.9 in the temporal hemifields; $P < 0.001$) in this study population with an average MD of − 7.66 dB, i.e., patients with moderate glaucoma.

Thus, these abovementioned studies and ours suggest that glaucomatous changes are found earlier in the superior or superonasal regions of central VFs and that N/T of mfERG in the central 5° may be useful for detecting glaucomatous VF and the corresponding inferior or inferotemporal inner OCT changes at least until reaching the moderate stage of disease.

We also found statistically significant correlations between N/T and the average mRNFL thickness and between N/T and the MD of HFA 10 − 2 (Table 4). This may support that N/T of mfERG can detect general functional and structural losses in the macular region in glaucoma. However, topical correlations between VF parameters and OCT measurements are stronger than those between N/T and VF parameters or OCT measurements. To improve the associations of N/T with OCT parameters and MT, identical measurement areas of N/T should be adapted in future research.

The PhNR amplitudes of the focal macular ERG scans can be used to assess the damages of the RGCs in glaucoma and the decrease in the PhNR amplitudes was associated with reductions in the cpRNFL and mRNFL thicknesses [6, 13]. The amplitudes of the PhNR of the focal ERG scans and PhNR/B correlated with the corresponding cpRNFL thicknesses when measured by scanning laser polarimetry in the

superotemporal and inferotemporal regions [21]. In the current study, mfPhNR/B measured by mfERG was significantly different between normal subjects and glaucoma patients (Table 2). We also found that the mfPhNR/B was significantly correlated with MT in all corresponding areas except for in the inferotemporal VF area (Table 5). However, among sectorial values of mfPhNR/B, significant correlation was found only between the central region of mfPhNR/B and the average mRNFL (Table 6). One of the reasons for this may be regional disagreement in the measurement areas. Machide et al. also found that the PhNRs of focal ERG were well-correlated with the GCC thickness within the central macula [5]. Kaneko et al. used mfERG to assess the PhNR recorded from five macular retinal locations and found selective reductions in the mfERG component only present within the central 15 degrees. Thus, another possibility is that the PhNR/B may be most useful within the central macula because of the highest RGC density being in the macula [15]. A multifocal technique could assess multiple independent stimulus locations simultaneously; however, the best way to go about topographic analysis has not yet been elucidated [22].

Although N/T and mfPhNR/B induced by mfERG showed correlations with MT and OCT parameters in several regions, no correlation was observed between the N/T and the sectorial values of mfPhNR/B in individual glaucoma patients (Table 7). There are several reasons for this. First, the stimulated areas of the retina do not completely correspond with each other. When we compared mfPhNR/B in the central or N/T and MT of HFA 10 − 2, significant correlations were observed, respectively (P=0.015; r□0.376 and P□0.003; r□−0.452). Additionally, when we compared mfPhNR/B in the central or N/T and central MT of HFA 30 − 2, significant correlations were observed, respectively (P□0.006; r□0.421 and P□0.009; r□−0.405). At least a moderate correlation was observed between respective ERG parameters and MT. Second, while the mfPhNR/B mainly reflects the anatomical loss of RGCs induced by glaucoma, N/T may reflect the disturbance ratio based on the difference in RGC distribution density between nasal and temporal areas. Both parameters may be used rather complementarily.

In our study, correlations between VF parameters and the N/T or mfPhNR/B were found to some extent. However, these correlation coefficients were weaker than those between VF and OCT parameters. The utility of the N/T and mfPhNR/B is substantially lower than OCT measurements. OCT measurement is a fast and completely noninvasive test. The best way to go about topographic analysis of mfERG parameters has not yet been proven and further study is required regarding whether mfERG parameters in conjunction with OCT measurements in the corresponding macular region may enhance diagnostic sensitivity in glaucoma.

Our study has several limitations. First, in normal subjects, we only measured mfERG for the purposes of direct comparison. Second, the effects of refractive error were not considered, and there were significant differences in refraction between normal participants and glaucoma patients. Myopia is a significant risk factor for OAG [23]; however, research has shown that only high myopia can affect the amplitudes of the first- and second-order kernels of the mfERG scans [24]. Although we excluded OAG patients with refractive errors of less than − 6.00 D, the mfERG responses in this study need to be carefully interpreted.

5. Conclusions

The N/T of the second-order kernel and the mfPhNR/B significantly correlate with the central sensitivity values as measured by automated perimetry and with morphological macular changes determined by OCT to some extent, although collation coefficients were smaller. Further investigations are needed to demonstrate whether N/T and mfPhNR/B should be used rather complementarily and ERG technology is a sensitive method for objective functional assessments in glaucomatous changes.

Abbreviations

mfERG
Multifocal electroretinography
MT
Mean thresholds
VF
Visual field
mRNFL
Macular retinal nerve fiber layer
GCIPL
Ganglion cell and inner plexiform layer
OCT
Optical coherence tomography
N/T
Nasal to temporal amplitudes ratio
mfPhNR/B
Multifocal photopic negative response to B-wave ratio
RGCs
Retinal ganglion cells
PhNR
Photopic negative response
PhNR/B
photopic negative response to B-wave ratio
ERG
Electroretinography
SAP
Standard automated perimetry
OAG
Open angle glaucoma
NTG
Normal tension glaucoma
IOPs
Intraocular pressures

POAG
Primary open-angle glaucoma
D
Diopters
VA
Visual acuity
logMAR
Logarithm of the minimum angle of resolution
RNFL
Retinal nerve fiber layer
HD-OCT
High-definition optical coherence tomography
cpRNFL
Circumpapillary retinal nerve fiber layer
GCA
Ganglion Cell Analysis
IPL
Inner plexiform layer
HFA
Humphrey Field Analyzer
HFA 30 − 2
Humphrey Field Analyzer with the Central 30 − 2 programs
HFA 10 − 2
Humphrey Field Analyzer with the Central 10 − 2 programs
VERIS
Visual Evoked Response Imaging System Science
CRT
Cathode ray tube
mfB-wave
Multifocal B-wave
MD
Mean deviation
PSD
Pattern standard deviation
GCC
Gganglion cell complex

Declarations

Acknowledgements

We would like to thank all of the participants involved in this study.

Funding: No funding was received for this research.

Contributions: KI and KM have made substantial contributions to conception and design, and interpretation of data; HT, KO and AS have made a substantial contribution to acquisition of data; HT, KI and KM have been involved in drafting the manuscript; TY provided critical revision; HT and KI performed the statistical analyses. All authors read and approved the final manuscript.

Ethics declarations

Ethics approval and consent to participate: The study followed the tenets of the Declaration of Helsinki and was approved by the Institutional Board of Research Associates of Gifu University Graduate School of Medicine. A written consent for participation was taken from each patient before the measurement.

Consent for publication: Not applicable

Competing interests: The authors declare that they have no competing interests

References

1. Viswanathan S, Frishman LJ, Robson JG, Harwerth RS, Smith EL 3rd. The photopic negative response of the macaque electroretinogram: reduction by experimental glaucoma. Invest Ophthalmol Vis Sci. 1999;40(6):1124-1136.
2. Drasdo N, Aldebasi YH, Chiti Z, Mortlock KE, Morgan JE, North The s-cone PHNR and pattern ERG in primary open angle glaucoma. Invest Ophthalmol Vis Sci. 2001;42(6):1266-1272.
3. Machida S, Tamada K, Oikawa T, Gotoh Y, Nishimura T, Kaneko M, Kurosaka D. Comparison of photopic negative response of full-field and focal electroretinograms in detecting glaucomatous eyes. J Ophthalmol. 2011;2011.pii:564131.
4. Falsini B, Marangoni D, Salgarello T, Stifano G, Montrone L, Campagna F, Alibert S,Balestrazzi E, Colotto A. Structure-function relationship in ocular hypertension and glaucoma: interindividual and interocular analysis by OCT and pattern ERG. Graefes Arch Clin Exp Ophthalmol. 2008;246(8):1153-1162.
5. Machida S, Kaneko M, Kurosaka D. Regional variations in correlation between photopic negative response of focal electoretinograms and ganglion cell complex in glaucoma. Curr Eye Res. 2015;40(4):439-449.
6. Machida S, Tamada K, Oikawa T, Yokoyama D, Kaneko M, Kurosaka D. Sensitivity and specificity of photopic negative response of focal electoretinogram to detect glaucomatous eyes. Br J Ophthalmol. 2010;94(2):202-208.
7. Viswanathan S, Frishman LJ, Robson JG, Walters JW. The photopic negative response of the flash electroretinogram in primary open angle glaucoma. Invest Ophthalmol Vis Sci. 2001;42(2):514-522.

8. Wang J, Cheng H, Hu YS, Tang RA, Frishman LJ. The photopic negative response of the flash electroretinogram in multiple sclerosis. Invest Ophthalmol Vis Sci. 2012;53(3):1315-1323.
9. Tang J, Edwards T, Crowston JG, Sarossy M. The Test-Retest Reliability of the Photopic Negative Response (PhNR). Transl Vis Sci Technol. 2014;3(6):1. eCollection 2.
10. Wu Z, Hadoux X, Hui F, Sarossy MG, Crowston JG. Photopic Negative Response Obtained Using a Handheld Electroretinogram Device: Determining the Optimal Measure and Repeatability. Transl Vis Sci Technol. 2016;5(4):8. eCollection
11. Asano E, Mochizuki K, Sawada A, Nagasaka E, Kondo Y, Yamamoto T. Decreased nasal-temporal asymmetry of the second-order kernel response of multifocal electroretinograms in eyes with normal-tension glaucoma. Jpn J Ophthalmol. 2007;51(5):379-389.
12. Takagi S, Tomita G, Nagasaka E, Eguchi S. Second-order component of multifocal electroretinogram in eyes with glaucoma. Rinsho Ganka (Jpn J Clin Ophthalmol). 2014;68:1427-1432.
13. Cvenkel B, Sustar M, Perovšek D. Ganglion cell loss in early glaucoma, as assessed by photopic negative response, pattern electroretinogram, and spectral-domain optical coherence tomography. Doc Ophthalmol. 2017;135(1):17-28.
14. Hori N, Komori S, Yamada H, Sawada A, Nomura Y, Mochizuki K, Yamamoto T. Assessment of macular function of glaucomatous eyes by multifocal electroretinograms. Doc Ophthalmol. 2012;125(3):235-247.
15. Kaneko M, Machida S, Hoshi Y, Kurosaka D. Alterations of photopic negative response of multifocal electroretinogram in patients with glaucoma. Curr Eye Res. 2015;40(1):77-86.
16. Lee WJ, Kim YK, Park KH, Jeoung JW. Trend-based Analysis of Ganglion Cell-Inner Plexiform Layer Thickness Changes on Optical Coherence Tomography in Glaucoma Progression. Ophthalmology. 2017;124(9):1383-1391.
17. Sutter EE and Tran D. The field topography of ERG components in man. 1. The photopic luminance response. Vision Res. 1992;32(3):433-446.
18. Van Astine AW, Viswanathan S. Test-retest reliability of the mutifocal photopic negative response. Doc Ophthalmol. 2017;134(1):25-36.
19. Ohkubo S, Higashide T, Udagawa S, Sugiyama K, Hangai M, Yoshimura N, Mayama C, Tomidokoro A, Araie M, Iwase A, et al. Focal relationship between structure and function within the central 10 degrees in glaucoma. Invest Ophthalmol Vis Sci. 2014;55(8):5269-5277.
20. Na JH, Sung KR, Lee JR, Lee KS, Baek S, Kim HK, Sohn YH. Detection of glaucomatous progression by spectral-domain optical coherence tomography. Ophthalmology. 2013;120(7):1388-1395.
21. Tamada K, Machida S, Oikawa T, Miyamoto H, Nishimura T, Kurosaka D. Correlation between photopic negative response of focal electroretinograms and local loss of retinal neurons in glaucoma. Curr Eye Res. 2010;35(2):155-164.
22. Wilsey LJ, Fortune B. Electroretinography in glaucoma diagnosis. Curr Opin Ophthalmol. 2016r;27(2):118-124

23. Suzuki Y, Iwase A, Araie M, Yamamoto T, Abe H, Shirato S, Kuwayama Y, Mishima HK, Shimizu H, Tomita G, et al. Risk factors for open-angle glaucoma in a Japanese population: the Tajimi Study. Ophthalmology. 2006;113(9):1613-1617.
24. Chen JC, Brown B, Schmid KL. Delayed mfERG responses in myopia. Vision Res. 2006;46(8-9):1221-1229.

Figures

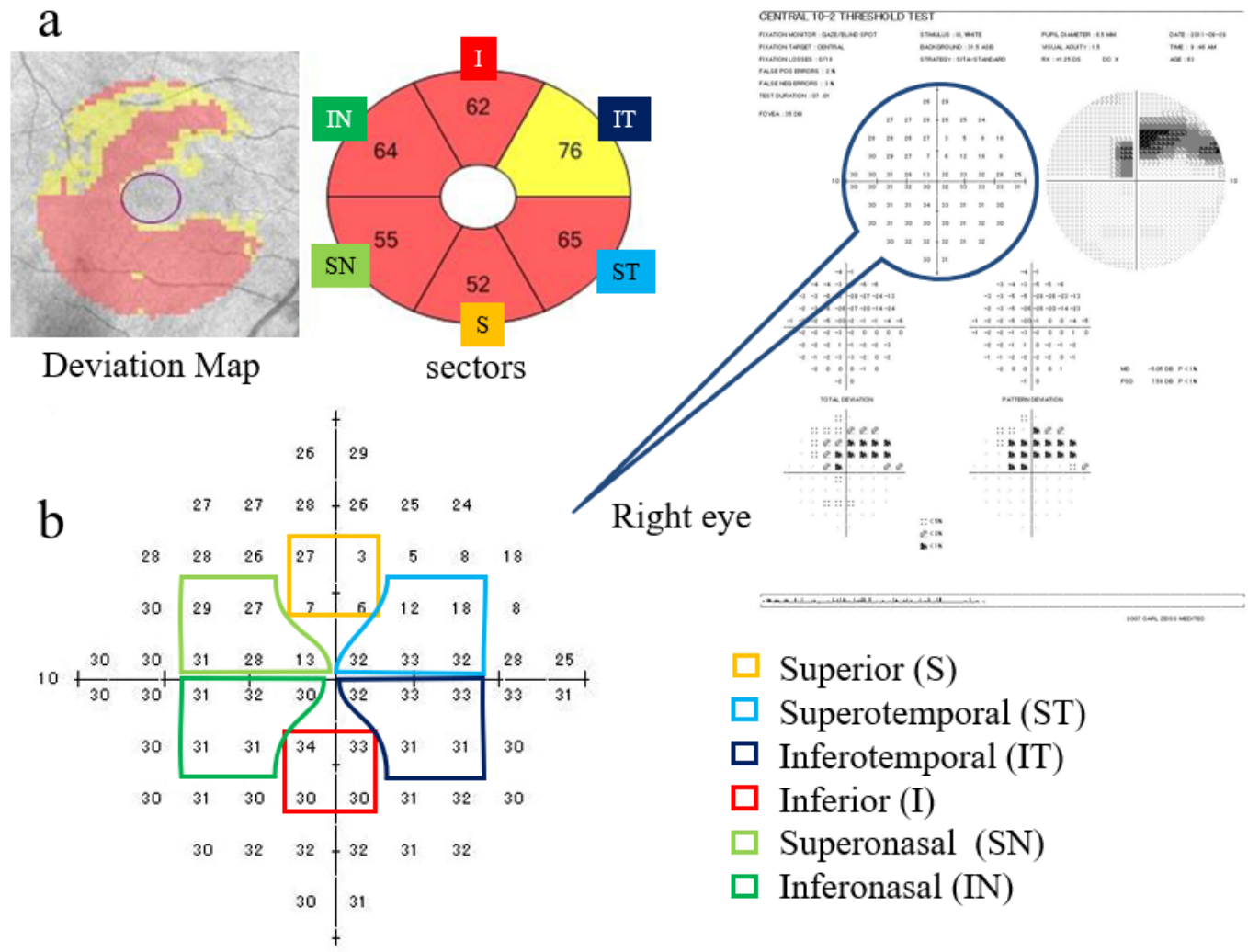

Figure 1

Association between optical coherence tomography (OCT) thickness and Humphrey Field Analyzer Central 10-2 program (HFA10-2) (a). The macular thickness is measured by OCT between two concentric circles of 2- and 6-mm diameters. (b) The findings of the HFA10-2 in right eye of glaucoma patient. Based on the retinal ganglion cell displacement [16], we classified the stimulus points on the HFA10-2 corresponding to the six sectors of the ganglion cell and inner plexiform layer (GCIPL) measurement

ellipse into 6 groups (i.e., superior, superotemporal, inferotemporal, inferior, superonasal, and inferonasal sectors).

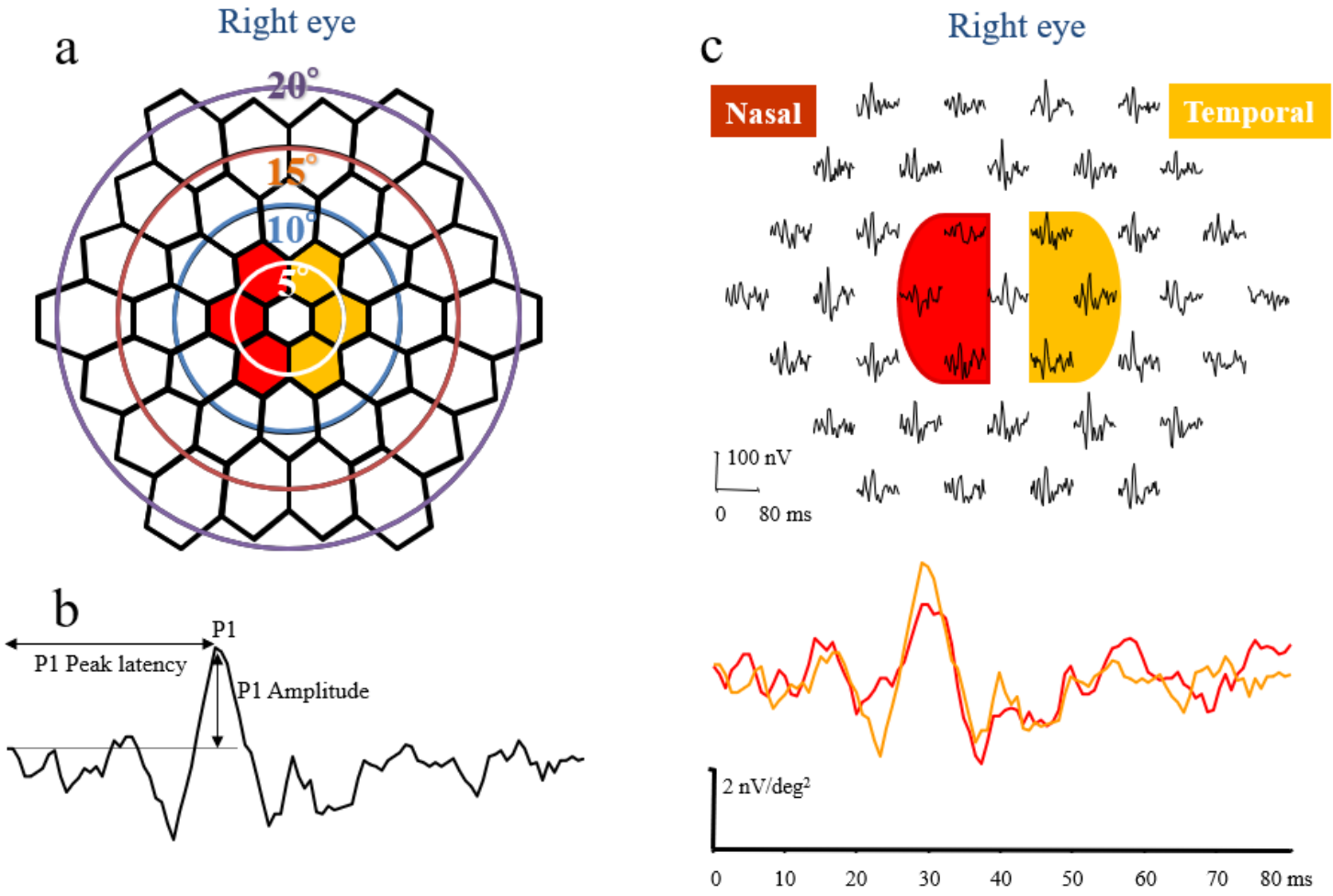

Figure 2

The stimulus array and the nasal to temporal amplitudes ratio obtained from multifocal electroretinograms (mfERGs) (a). The pattern of the 37-hexagon stimulus array with circles indicating radii of 5°, 10°, 15° and 20°in right eye. (b). The measurements of the first slice of the second-order kernels obtained from multifocal electroretinograms (mfERGs). The first positive peak, P1 amplitude was measured. (c). We separated the hexagons and averaged them according to the temporal (orange color) nasal (red color) hemispheres. We used the ratio of the amplitudes of the mfERGs of the nasal to the temporal hemisphere within the central 5° (N/T) to evaluate the asymmetry.

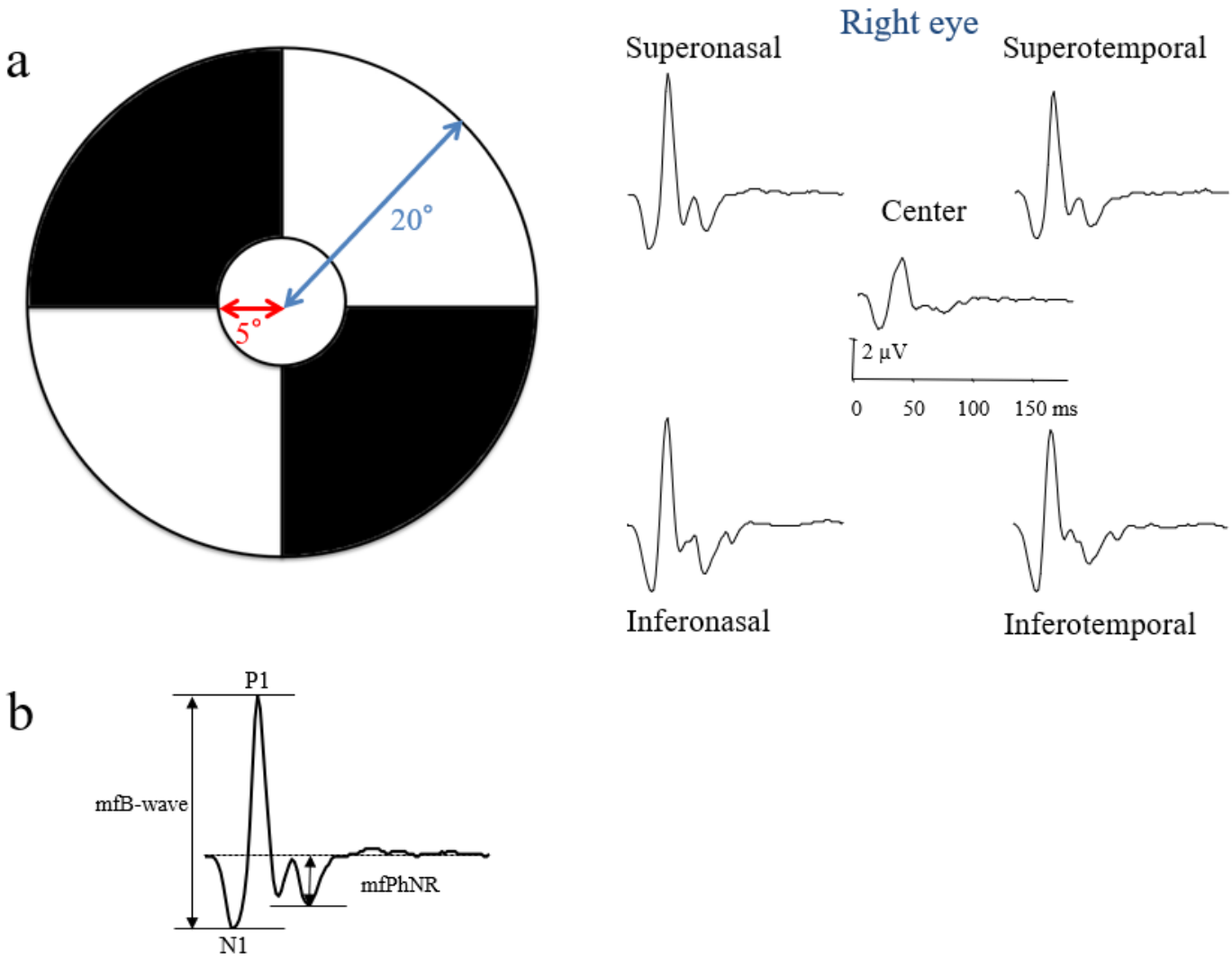

Figure 3

The stimulus patterns and the multifocal photopic negative response (mfPhNR) (a). The stimulus patterns (a circular stimulus with a 5° radius centered on the fovea and a quarter of an annulus placed in the superotemporal, superonasal, inferotemporal, and inferonasal regions around the fovea) were used to elicit mfERGs. The radius of the inner border of the annulus was 5° and that of the outer border was 20°. (b). The representative waveforms of the mfERGs recoded from five sectors in right eye of a patient with glaucoma. We measured the multifocal B-wave (mfB-wave; P1–N1) from the first negative trough to the peak of the following positive wave. The mfPhNR was measured from the baseline to the negative trough at more than 70 ms from the stimulus onset.

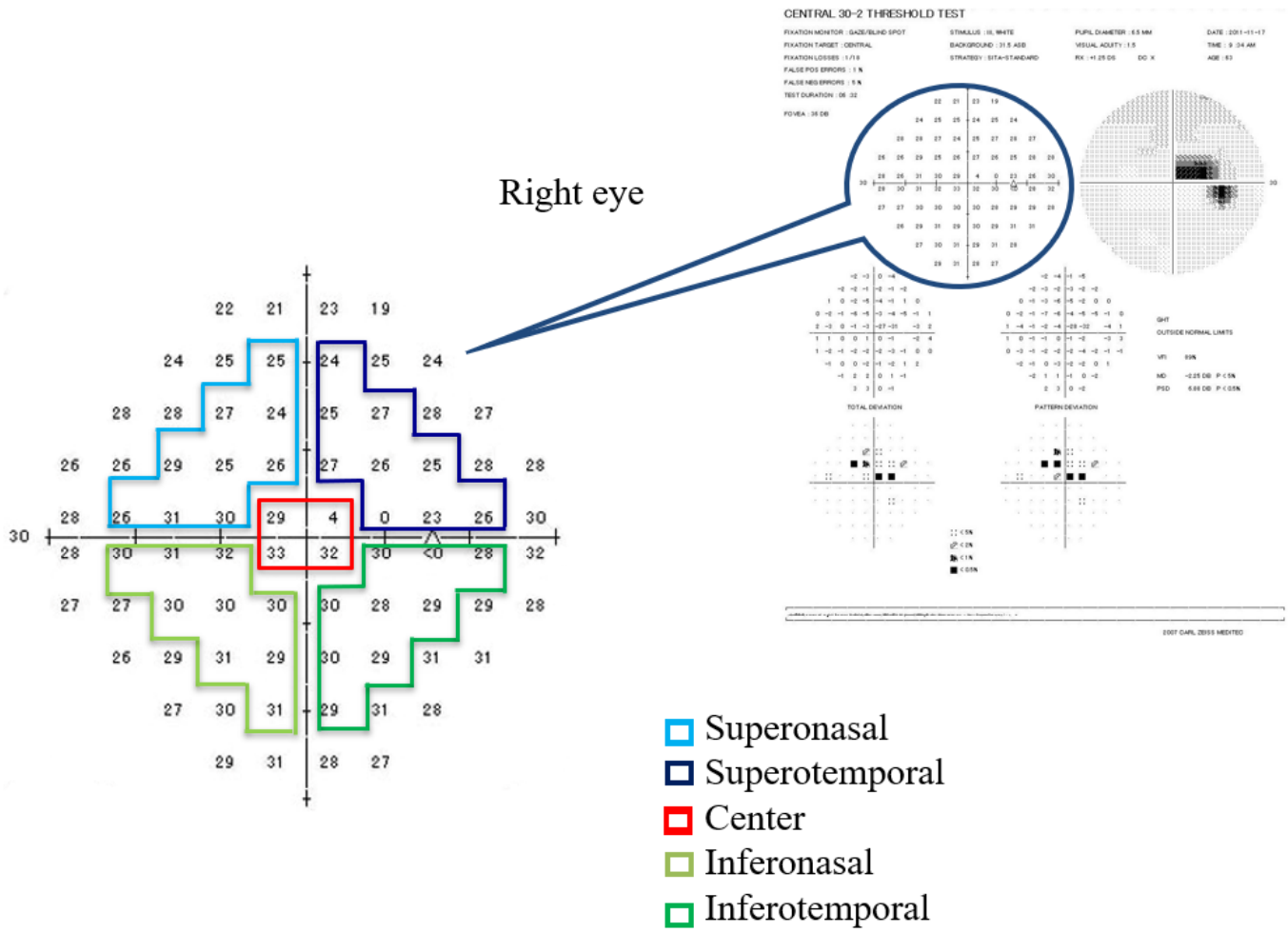

Figure 4

Humphrey Field Analyzer Central 30-2 program (HFA 30-2) corresponding to the mfPhNR regions. (see Figure 3). To compare the multifocal photopic negative response to B-wave ratio (mfPhNR/B) with the corresponding visual field findings, we measured the thresholds with the HFA 30-2 and averaged for the same sectors (i.e., superonasal, superotemporal, center, inferonasal, and inferotemporal) according to the distance from the macula within the central 20°.